

# Simulations of coronal shock acceleration in self-generated waves

R. Vainio,\* N. Agueda,\* T. Laitinen,† and M. Battarbee†

\**Department of Physics, FI-00014 University of Helsinki, Finland*

†*Department of Physics and Astronomy, FI-20014 University of Turku, Finland*

**Abstract.** We have developed a simulation model of particle acceleration in coronal shock waves. The model is based on a Monte Carlo method, where particles are traced in prescribed large-scale electromagnetic fields utilizing the guiding center approximation, and the effects of turbulence are employed via a scattering operator obtained from quasilinear theory. The scattering amplitude is directly proportional to the intensity of Alfvén waves at gyro-resonant wavenumbers. The wave intensity in our model is traced simultaneously with the particles. We trace an Alfvén wave field propagating outwards from the Sun using WKB propagation supplemented with a phenomenological wavenumber diffusion term and a growth rate computed from the net flux of the accelerated particles. We consider initial wave amplitudes small enough to allow a rapid escape of the particles from the shock to the ambient medium. Thus, the Alfvén waves responsible for the diffusive acceleration of particles are generated by the accelerated particles themselves in our model. Particle acceleration occurs in a coronal shock propagating at constant projected speed along the ambient magnetic field with a shock-normal angle that evolves during the simulation. We report on simulations where protons are accelerated up to about 80 MeV in a matter of 100 seconds, and present a scaling law implying that protons could be accelerated up to GeV energies in oblique and quasi-perpendicular coronal shocks.

**Keywords:** Solar energetic particles, Coronal shock acceleration, Self-generated turbulence

## I. INTRODUCTION

Large, long-duration solar energetic particle (SEP) events are believed to be accelerated in shock waves driven by coronal mass ejections (CMEs) [1]. The most plausible acceleration mechanism is diffusive shock acceleration (DSA), where particles gain energy by repeatedly crossing the compressive shock front [2]. In order to gain energy rapidly enough to account for the observations of rapid ion acceleration in the corona, particles need to be efficiently scattered by magnetic fluctuations around the shock (e.g., [3]). The turbulent magnetic fields, however, need to be limited to a relatively thin layer in front of the shock, because otherwise the particles are not able to escape to the ambient medium and be detected at 1 AU some tens of minutes after the onset of the related solar flare (e.g., [4]). Such a

turbulent layer may be generated by Alfvén waves driven unstable by the accelerated particles streaming away from the shock [2]. We refer to this kind of acceleration as DSA-SGW (DSA in self-generated waves).

There are several numerical methods to simulate DSA-SGW in coronal and interplanetary shocks. The simplest class of models relies on analytical estimates of the quasi-steady-state ion spectra that are accelerated at the shock and transported numerically both upstream and downstream of the shock [5], [6]. These models do not, however, compute particle escape from the turbulent shock self-consistently. Analytical models for the self-consistent particle escape have been proposed, and they are based either on time-dependence of the wave-growth process [7] or to the effect of adiabatic focusing of particles in the diverging mean magnetic field [8]. Time-dependent, fully kinetic models of the process that self-consistently employ these effects have also been developed for modeling ion acceleration in parallel coronal shock waves self-consistently [9], [10], [12]. In this paper we extend our earlier simulation model (presented in [9], [10]) to coronal shocks propagating at oblique (and quasi-perpendicular) angles relative to the shock front.

## II. THE MODEL

Our kinetic model of DSA-SGW ([9], [10]) relies on the Monte Carlo (MC) method (see, e.g., [4]) to compute particle transport in prescribed large-scale electromagnetic fields appended with a scattering operator employing the effects of the turbulent field components. According to quasi-linear theory the particle scattering frequency is proportional to the power spectrum of the Alfvén waves,  $P(k)$ , at the resonant wavenumber  $k = m\Omega_0/p\mu$ , where  $\Omega_0 = qB/mc$  is the cyclotron frequency of particles with charge  $q$  and mass  $m$  in a magnetic field  $B$ ,  $c$  is the speed of light, and  $p$  and  $\mu$  are the momentum and the pitch-angle cosine of the particle, as measured in the frame moving with the phase speed of the scattering waves. In our simulation model [9], [10], we neglect the dependence of the resonant  $k$  on  $\mu$ , which means that there is a one-to-one correspondence (at constant  $B$ ) between the particle rigidity  $R = pc/q$  and the resonant wavenumber,  $k = B/R$ . This approximation leads to an isotropic scattering frequency,  $\nu = \frac{\pi}{2}\Omega |k|P(k)/B^2$ , which is computationally much more efficient than a general scattering operator, where the scattering frequency may depend (arbitrarily) on pitch

angle. (Here,  $\Omega = \Omega_0/\gamma$  is the relativistic gyrofrequency and  $\gamma$  is the Lorentz factor of the particle.)

We model the wave–particle interaction process self-consistently in the sense that we also update the intensity of the scattering waves during the interaction. The growth rate of the waves is computed from the accelerated protons that we trace. Using the same approximation of  $k = B/R$  as when computing the scattering rate of the protons, the growth rate of the waves can be obtained as  $\sigma(k) = (\pi/2) \Omega_{0,p} (pS_p/nv_A)_{p=m_p\Omega_{0,p}/k}$ . Here,  $m_p$  and  $\Omega_{0,p}$  are the proton mass and cyclotron frequency,  $n$  and  $v_A$  are the electron density and the Alfvén speed of the plasma, and  $S_p = 2\pi p^2 \int_{-1}^{+1} v\mu F d\mu$ ,  $v$ , and  $F$  are the proton streaming per unit momentum, proton speed, and proton distribution function, respectively. In addition to wave growth, we include the WKB-propagation of the waves along the field lines and employ a wavenumber diffusion term that mimics the effects of turbulent cascading. Since WKB transport occurs at constant wave frequency,  $f = V|k|/2\pi$ , where  $V$  is the phase speed of the waves in the inertial frame, we use  $f$  instead of  $k$  as the independent variable in our simulations. We assume that  $V = u + v_A$ , where  $u$  is the solar wind speed, and that  $V$  is constant inside the simulation domain.

The wave simulation domain consists of a 2-D grid with one spatial dimension (radial) and frequency. We consider a model, where particles and waves are confined to a single flux tube around a radial field line with an over-expanding cross-sectional area,  $A(r) \propto B^{-1}$ . The magnetic field magnitude inside the flux tube scales like  $B \propto r^{-2}[1 + b_f(R_\odot/r)^6]$ , where  $b_f$  is a parameter which we set to 1.9. The wave field is initialized by computing the intensity in the box without any wave growth and assuming that the source of the waves is at the surface of the Sun. The initial wave field intensity is fixed by assuming that the spectrum at the solar surface is  $\propto f^{-1}$  and that the scattering mean free path,  $v/\nu$ , of 100-keV protons is  $1 R_\odot$  at  $r = 1.5 R_\odot$ . This corresponds to a wave intensity (per logarithmic bandwidth) of  $6 \times 10^{-7} B^2$  at the solar surface.

The simulations commence so that low-energy particles are injected to the simulation at the shock wave, as the shock propagates from an initial radial distance of 1.5 solar radii outwards at a constant speed  $V_s$  along a magnetic field line, and with constant density and magnetic-field compression ratios,  $X$  and  $X_B$ . The simulation grid is Lagrangian in the sense that it is moved at speed  $V$  outwards from the Sun. This makes it easy to compute the wave-frame streaming of energetic particles, needed for the wave growth, by simply counting the number particles per unit time crossing the grid cell boundaries in the spatial direction.

The shock in the simulation is treated as an inner boundary condition that moves outwards relative to the grid at speed  $V_s - V$ . The waves are simply overtaken by the shock. Particle–shock interaction is treated adiabatically in the de Hoffmann – Teller (HT) frame, i.e.,

incident particles with small enough pitch-cosine ( $\mu^2 < 1 - X_B^{-1}$  in HT frame) are elastically reflected by the shock. Those particles that are transmitted downstream are immediately brought back to the shock and their weight in the simulation is decreased by multiplying it with the probability of return  $\mathcal{P}_{\text{ret}} = (v - u_2)^2/(v + u_2)^2$ , where  $u_2$  is the downstream flow speed (in the HT frame) and  $v$  is measured in the downstream rest frame. The downstream scattering process responsible for bringing the particles back to the shock is assumed to be very fast and elastic in the rest frame of the fluid. Note that this probability of return is most accurate at velocities  $v \gg V_s$ , where the distribution function can be assumed to be quasi-isotropic.

### III. SIMULATION RESULTS

We consider three simulation scenarios with different projected shock speeds and compression ratios: (A)  $V_s = 1000 \text{ km s}^{-1}$ ,  $X = 4$ ,  $X_B = 1$ ; (B)  $V_s = 3000 \text{ km s}^{-1}$ ,  $X = 3.74$ ,  $X_B = 3.71$ ; and (C)  $V_s = 10000 \text{ km s}^{-1}$ ,  $X = 3.63$ ,  $X_B = 3.63$ . These correspond to a fast-mode shock propagating into a cold medium with an Alfvén speed of  $400 \text{ km s}^{-1}$  at a shock-normal speed of  $1000 \text{ km s}^{-1}$  and a shock-normal angle of  $\theta_{Bn} = 0^\circ$ ,  $\theta_{Bn} \approx 70^\circ$ , and  $\theta_{Bn} \approx 84^\circ$ , respectively. In all cases, we inject particles with a uniform distribution in radial direction (corresponding to the density of seed particles inversely proportional to the flux-tube cross-sectional area). The speed of the injected particles in the frame of the shock is the shock speed plus an exponentially deviated random component with a mean value of  $375 \text{ km s}^{-1}$ . The particle propagation direction is obtained from a flux-weighted isotropic distribution in the outward half-space. Thus, the injection does not correspond to any self-consistent injection model, but an injection momentum scaling with the fluid speed in the HT frame is a reasonable assumption, if the injection is related to reflection from the shock [11]. The total number of particles injected into the acceleration process for Cases A–C is taken to be  $N_{\text{inj}} = 3 \times 10^{34}$  per steradian, but for Case (A) we have also considered a run with  $N_{\text{inj}} = 3 \times 10^{35}$  (Case A') and for Case (B) a run with  $N_{\text{inj}} = 10^{35}$  per steradian (Case B'). These primed runs together with run C, thus, correspond to cases where the number of injected particles is inversely proportional to the projected shock speed along the magnetic field. We take the also simulation time  $t_{\text{max}}$  to be inversely proportional to the projected shock speed, so that the shock propagates a distance of  $V_s t_{\text{max}} = 10^6 \text{ km}$  along the field line in each case. Note that all our runs correspond to an injection rate that is a very small fraction of the total number of particles overtaken by the shock, which is about  $8 \times 10^{40}$  particles per sr at the solar surface.

The results of the Cases A and A' agree perfectly with the results of our previous simulation code [9], [10], where the shock was always parallel. For the adopted low injection rate, the parallel shock is able

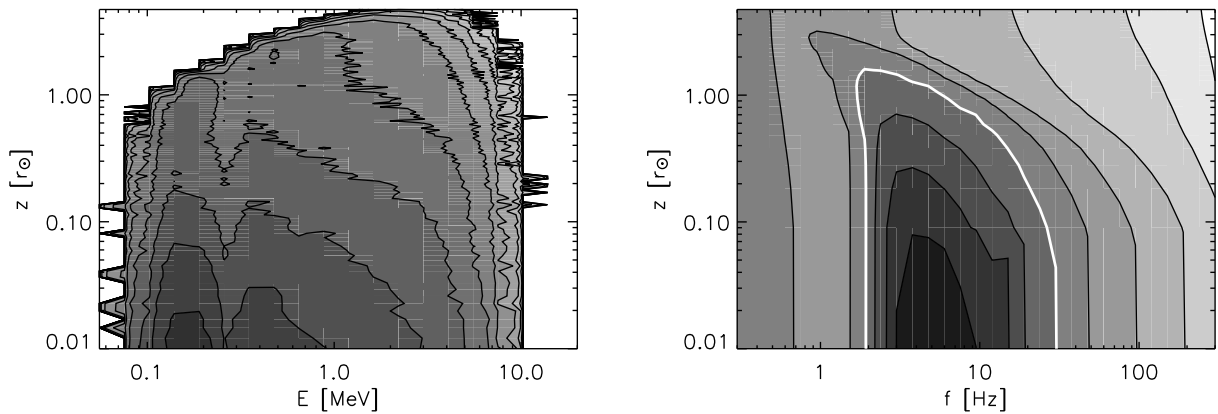


Fig. 1. Contour plots of the energetic particle energy spectrum (left) and the self-generated Alfvén-wave frequency spectrum (right) for Case B (see text for details), as a function of distance ( $z$ ) from the shock, in the end of the simulation run ( $t = 333.3$  s). Contour level separation is half an order of magnitude. The wave spectrum on the right is given as divided by the WKB wave spectrum corresponding to the same initial and boundary conditions as used in the simulation. The white contour is at the unit level.

to accelerate particles only up to about 200 keV in Case A and somewhat above 1 MeV in Case A'. For the oblique (Cases B and B') and quasi-perpendicular (Case C) simulations, however, new interesting results are obtained. For Case B, we obtain a maximum energy of about 10 MeV in a simulation time corresponding to the same propagation distance along the field as for the parallel shock. For Case B' we obtain a maximum energy of about 50 MeV and for Case C about 80 MeV. The Alfvén waves grow in the simulations by several orders of magnitude as a result of proton streaming away from the Sun. The proton spectrum and the spectrum of the Alfvén waves are plotted in Fig. 1 for Case B. The maximum wave intensities correspond to values of about two to three orders of magnitude above the WKB spectrum, i.e., they are still well below  $\delta B^2/B^2 = 10^{-3}$  per unit logarithmic bandwidth in all cases.

#### IV. DISCUSSION AND CONCLUSION

For DSA-SGW in a parallel shock, we derived in [9] an equation for the cutoff momentum in the spectrum,  $p_c$ , as a function of shock and injection parameters as

$$p_c(t_{\max}) = p_0 \left( 1 + \delta \frac{(V_s - V) t_{\max}}{X_k h} \right)^{(X_k - 1)/3}, \quad (1)$$

where  $p_0$  is the injection momentum (which scales like  $V_s$  in our model),  $\delta$  is a numerical factor of the order unity, and  $X_k$  is the scattering-center compression ratio [13] of the shock. Furthermore,  $h = (2/\pi\beta\varepsilon)(v_A/\Omega_{0,p})$ ,  $\beta = 3X_k/(X_k - 1)$ , and  $\varepsilon$  is the normalized injection rate, i.e., the injection rate is

$$Q = \frac{N_{\text{inj}}}{A(r) t_{\max}} = \varepsilon u_1 n, \quad (2)$$

where  $u_1$  is the plasma flow speed from the upstream to the shock in the HT frame and  $n$  is the number density of the bulk plasma. Note that in our density and magnetic field model,  $h$  is approximately constant in the corona [9].

For an oblique shock, the calculation of the maximum momentum proceeds very similarly as in the case of a parallel shock. The mean particle momentum gain per one interaction with an oblique shock is  $\Delta p = 4(p/v)u_1(X - 1)/(3X)$ , if wave propagation is neglected, i.e., if  $X_k = X$  [14]. The mean residence time of particles in the upstream region between the shock crossings is as in the parallel shock case, but recalling that the relevant speed of the shock is now the one projected along the magnetic field. Thus, a good estimate of the maximum momentum is obtained by simply taking the values of the shock speed, the wave speed and the bulk flow speed as the ones projected along the magnetic field in Eq. (1). This gives a rough scaling law of

$$p_c(t_{\max}) \propto p_0 N_{\text{inj}}^{(X_k - 1)/3}, \quad (3)$$

which our simulations seem to obey relatively well for the few cases considered. Since we take into account the finite speed of the scattering waves relative to the plasma in the upstream region but ignore it in the downstream region, we have  $X_k = (V_s - V) \cos \psi_1 / (u_2 \cos \psi_2) = X(V_s - V)/(V_s - u)$ , where  $\psi$  is the angle between the shock normal and the magnetic field. The value of the exponent is  $(X_k - 1)/3 \approx 0.49$  in Cases A and A', 0.76 in cases B and B', and 0.83 in Case C in the end of the runs.

The scaling law (3) predicts that oblique and quasi-perpendicular shocks may accelerate particles to high energies rather efficiently without pumping the waves to non-linear amplitudes. By increasing the number of injected particles by another factor of three relative to Case B', our scaling law predicts acceleration up to  $\sim 250$  MeV, while the wave spectrum stays still well below non-linear amplitudes. (The wave spectrum at the shock at the wavenumber resonant with  $p_c$  can be shown to scale roughly like  $N_{\text{inj}}^{(2X_k - 5)/3}$ , if  $p_0 \propto V_s$  and  $p_c < mc$ .) In Case C, a factor of three in the number

of injected ions would lead to acceleration up to GV rigidities, i.e., close to the GLE limit. There is no reason to believe that relativistic energies could not be achieved in our model.

The obtained scaling law (3) would have to be explored in more detail using a much larger number of runs extending to higher energies, before definite conclusions about GLE energies from shocks can be drawn. Such runs, however, would require at least an order of magnitude longer running times than the ones presented in this paper, since the time step in our simulation is inversely proportional to the wave intensity (which goes up) and since the spatial resolution of the grid is proportional to  $h$  (which goes down) and this further decreases the time step and leads to a need of increased particle statistics. We have started to expand the data base of the simulation results with such runs, and they will be presented in another paper in near future.

Finally, we point out that our particle propagator does not include perpendicular transport, which limits its use to cases with  $\tan^2 \psi_1 \ll \kappa_{\parallel} / \kappa_{\perp}$ , where  $\kappa_{\parallel}$  and  $\kappa_{\perp}$  are the diffusion coefficients parallel and perpendicular to the mean field, respectively. Thus, particle acceleration in nearly perpendicular shocks would in fact have to be treated with a more general model of particle transport.

*Acknowledgements:* The academy of Finland is thanked for financial support (projects 121650 and 124837).

#### REFERENCES

- [1] Reames, D. V. 1999, *Space Sci. Rev.*, 90, 413
- [2] Bell, A. R. 1978, *MNRAS*, 182, 147
- [3] Vainio, R. 2009, in: *Proc. IAU Symposium No. 257*, 413, doi:10.1017/S1743921309029640
- [4] Vainio, R., Kocharov, L., Laitinen, T. 2000, *ApJ*, 528, 1015
- [5] Zank, G. P., Rice, W. K. M., Wu, C. C. 2000, *JGR*, 105, 25,079
- [6] Rice, W. K. M., Zank, G. P., Li, G. 2003, *JGR*, 108, 1369
- [7] Vainio, R. 2003, *A&A*, 406, 735
- [8] Lee, M. A. 2005, *ApJS*, 158, 38
- [9] Vainio, R., Laitinen, T. 2007, *ApJ*, 658, 622
- [10] Vainio, R., Laitinen, T. 2008, *J. Atm. Solar-Terr. Phys.*, 70, 467
- [11] Sandroos, A., Vainio, R. 2009, *ApJS*, 181, 183
- [12] Ng, C. K., Reames, D. V. 2008, *ApJ*, 686, L123
- [13] Vainio, R., Schlickeiser, R. 1998, *A&A*, 331, 793
- [14] Drury, L.O'C. 1983, *Rep. Prog. Phys.*, 46, 973